

## Neutral-Ligand Complexes of Bis(imino)pyridine Iron: Synthesis, Structure, and Spectroscopy

Suzanne C. Bart,<sup>†</sup> Emil Lobkovsky,<sup>†</sup> Eckhard Bill,<sup>‡</sup> Karl Wieghardt,<sup>‡</sup> and Paul J. Chirik<sup>\*†</sup>*Department of Chemistry and Chemical Biology, Baker Laboratory, Cornell University, Ithaca, New York 14853, and Max-Planck Institute of Bioinorganic Chemistry, Stiftstrasse 34-36, D-45470 Mülheim an der Ruhr, Germany*

Received May 5, 2007

A family of bis(imino)pyridine iron neutral-ligand derivatives,  $(^i\text{PrPDI})\text{FeL}_n$  ( $^i\text{PrPDI} = 2,6\text{-(2,6-}^i\text{Pr}_2\text{-C}_6\text{H}_3\text{N=CMe)}_2\text{C}_6\text{H}_3\text{N}$ ), has been synthesized from the corresponding bis(dinitrogen) complex,  $(^i\text{PrPDI})\text{Fe}(\text{N}_2)_2$ . When L is a strong-field ligand such as  $^i\text{BuNC}$  or a chelating alkyl diphosphine such as DEPE (DEPE = 1,2-bis(diethylphosphino)ethane), a five-coordinate, diamagnetic compound results with no spectroscopic evidence for mixing of paramagnetic states. Reducing the field strength of the neutral donor to principally  $\sigma$ -type ligands such as  $^i\text{BuNH}_2$  or THT (THT = tetrahydrothiophene) also yielded diamagnetic compounds. However, the  $^1\text{H}$  NMR chemical shifts of the in-plane bis(imino)pyridine hydrogens exhibit a large chemical shift dispersion indicative of temperature-independent paramagnetism (TIP) arising from mixing of an  $S = 1$  excited state via spin–orbit coupling. Metrical data from X-ray diffraction establish bis(imino)pyridine chelate reduction for each structural type, while Mössbauer parameters and NMR spectroscopic data differentiate the spin states of the iron and identify contributions from paramagnetic excited states.

## Introduction

Bis(imino)pyridine ligands have attracted considerable attention due to their ease of synthesis, steric and electronic modularity, and well-documented ability to support a range of catalytically active metal centers and other interesting structural types.<sup>1</sup> One notable feature of this ligand class is its redox activity,<sup>2</sup> the ability to accept three electrons in the  $\pi$ -system of the terdentate chelate.<sup>3</sup> As noted by Gambarotta, Budzelaar, and co-workers, this phenomenon stabilizes reduced compounds whose low oxidation state assignment is often deceiving.<sup>4</sup>

Ligand-centered redox activity is particularly important in reduced bis(imino)pyridine iron compounds. The square-

planar iron chloride and methyl complexes,  $(^i\text{PrPDI})\text{FeX-} (^i\text{PrPDI} = 2,6\text{-(2,6-}^i\text{Pr}_2\text{C}_6\text{H}_3\text{NCMe)}_2\text{C}_5\text{H}_3\text{N}$ ;  $\text{X} = \text{Cl}, \text{CH}_3$ ),<sup>5</sup> exhibit Mössbauer isomer shifts, X-ray metrical parameters, and magnetic properties consistent with a high spin-ferrous ion antiferromagnetically coupled to a monoreduced chelate,  $[\text{PDI}]^-$  (Figure 1).<sup>6</sup> This description of the electronic structure has been corroborated by DFT calculations where the computed optimized structures successfully reproduce both the X-ray data and the Mössbauer isomer shifts. Continued reduction in the presence of neutral donors such as dinitrogen, carbon monoxide, or 4-(dimethylamino)pyridine (DMAP) furnished the corresponding  $(^i\text{PrPDI})\text{FeL}_n$  derivatives.<sup>6,7</sup> For these compounds, computational, spectroscopic, and structural data support an intermediate-spin ferrous ion complexed by a dianionic  $[\text{PDI}]^{2-}$  chelate (Figure 1). A similar electronic structure assignment has been suggested by Gambarotta and co-workers for the square planar bis(imino)pyridine iron methyl anion,  $[(^i\text{PrPDI})\text{FeMe}]^-$ .<sup>8</sup>

\* To whom correspondence should be addressed. E-mail: pc92@cornell.edu.

<sup>†</sup> Cornell University.

<sup>‡</sup> Max-Planck Institute of Bioinorganic Chemistry.

(1) Bianchini, C.; Giambastiani, G.; Rios, I. G.; Mantovani, G.; Meli, A.; Segarra, A. M. *Coord. Chem. Rev.* **2006**, *250*, 1391.

(2) de Bruin, B.; Bill, E.; Bothe, E.; Weyhermüller, T.; Wieghardt, K. *Inorg. Chem.* **2000**, *39*, 2936.

(3) Enright, D.; Gambarotta, S.; Yap, G. P. A.; Budzelaar, P. H. M. *Angew. Chem., Int. Ed.* **2002**, *41*, 3873.

(4) Scott, J.; Gambarotta, S.; Korobkov, I.; Knijnenburg, Q.; de Bruin, B.; Budzelaar, P. H. M. *J. Am. Chem. Soc.* **2005**, *127*, 17204.

(5) Bouwkamp, M. W.; Bart, S. C.; Hawrelak, E. J.; Trovitch, R. J.; Lobkovsky, E.; Chirik, P. J. *Chem. Commun.* **2005**, 3406.

(6) Bart, S. C.; Chlopek, K.; Bill, E.; Bouwkamp, M. W.; Lobkovsky, E.; Neese, F.; Wieghardt, K.; Chirik, P. J. *J. Am. Chem. Soc.* **2006**, *128*, 13901.

(7) Knijnenburg, Q.; Gambarotta, S.; Budzelaar, P. H. M. *Dalton Trans.* **2006**, *46*, 5442.

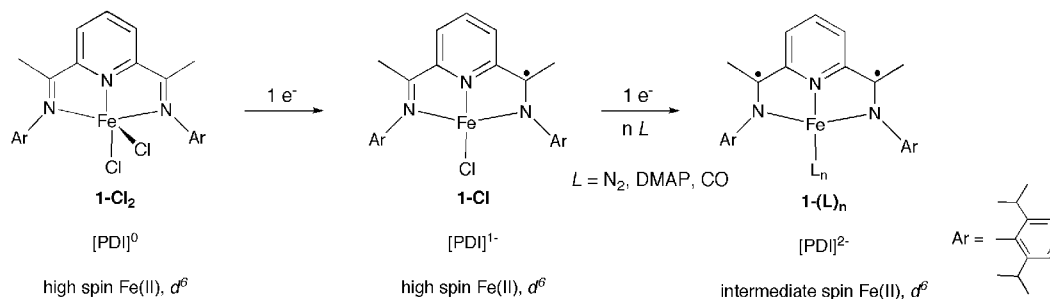


**Figure 1.** Ligand-centered reductions in bis(imino)pyridine iron compounds.

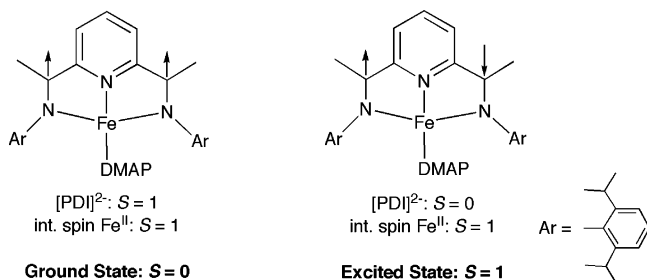


**Figure 2.** Electronic structure and the origin of temperature-independent paramagnetism in **1-DMAP**.

The  $^1\text{H}$  NMR spectrum of the bis(imino)pyridine iron DMAP derivative,  $(^{\text{iPr}}\text{PDI})\text{Fe}(\text{DMAP})$  (**1-DMAP**), is similar to isoelectronic  $(^{\text{iPr}}\text{PDI})\text{CoMe}^9$  and provides additional insight into the electronic structure of the compound. While the hydrogens on the orthogonal aryl substituents appear close to their diamagnetic reference values (e.g., those in the free  $^{\text{iPr}}\text{PDI}$  ligand), the protons in the iron–chelate plane are shifted dramatically. The origin of this behavior is temperature-independent paramagnetism (TIP), whereby an energetically similar  $S = 1$  excited-state mixes into the  $S = 0$  ground state via spin–orbit coupling or antisymmetric exchange.<sup>7</sup> Results of DFT calculations establish intermediate-spin ( $S_{\text{Fe}} = 1$ ) ferrous ions in both the ground and excited states.<sup>6</sup> The only difference in the electronic configuration lies in the spin state of the bis(imino)pyridine dianion. In the ground state, a triplet diradical dianion ( $S_{\text{L}} = 1$ ) is antiferromagnetically coupled to the ferrous ion, while in the excited state, the ligand is a singlet diradical ( $S_{\text{L}} = 0$ ) (Figure 2). Coupling of the two electrons occurs through a metal d orbital, in agreement with predictions by the Goodenough–Kanamori rules.<sup>10</sup> This description of the electronic structure is distinct from the iron bis(dinitrogen) complex reported by Danopoulos and co-workers where the imines have been replaced by *N*-heterocyclic carbenes and there is no evidence for chelate reduction.<sup>11</sup>

The redox activity of the bis(imino)pyridine chelate appears to play an important role in the catalytic activity of

the resulting iron compounds. The bis(dinitrogen) precursor,  $(^{\text{iPr}}\text{PDI})\text{Fe}(\text{N}_2)_2$  (**1-(N<sub>2</sub>)<sub>2</sub>**),<sup>12</sup> has been shown to be an effective pre-catalyst for the intramolecular  $[2\pi + 2\pi]$  cyclization of  $\alpha,\omega$ -dienes to yield the corresponding bicycloheptane derivatives as a single isomer.<sup>13</sup> Preliminary mechanistic studies involving model compounds support a pathway whereby the ferrous oxidation state is maintained throughout the catalytic cycle, obviating complications from metal deposition arising from formal reductive elimination and generation of  $\text{M}(0)$  species (Figure 3).<sup>14</sup>

Redox-active bis(imino)pyridines have also been shown to impart unique reactivity into iron–nitrogen bonds.<sup>15</sup> Treatment of **1-(N<sub>2</sub>)<sub>2</sub>** with 1 equiv of an aryl azide results in a net two-electron oxidation to yield a family of  $(^{\text{iPr}}\text{PDI})\text{Fe}=\text{NAr}$  compounds ( $\text{Ar}$  = substituted aryl).<sup>16</sup> A combination of X-ray diffraction, zero-field Mössbauer experiments, and SQUID magnetization studies established an overall  $S = 1$  complex with an intermediate-spin ferric ion ( $S_{\text{Fe}} = 3/2$ ) antiferromagnetically coupled to a bis(imino)pyridine monoanion,  $[\text{iPrPDI}]^-$  ( $S_{\text{L}} = 1/2$ ). This electronic structure translates onto the reactivity of this family of compounds, as complete hydrogenation of the iron–nitrogen linkage to yield the corresponding free aniline was observed. Similar hydrogenative N–N bond cleavage has also been observed with related diazoalkane derivatives.<sup>17</sup>

In this contribution, we further explore the role of TIP in bis(imino)pyridine iron compounds bearing neutral ligands as a function of the donor. Studies of this type may ultimately prove essential in understanding the electronic structure of key intermediates during catalytic turnover. The results of this combined synthetic and spectroscopic study establish a correlation between the field strength of the neutral donor, spin state of the iron, and the degree of contribution from the excited state.

## Results and Discussion

**Synthesis and Solution Characterization.** The iron bis(dinitrogen) complex, **1-(N<sub>2</sub>)<sub>2</sub>**, was treated with the appropri-

- (8) Scott, J.; Gambarotta, S.; Korobkov, I.; Budzelaar, P. H. M. *Organometallics* **2005**, *24*, 6298.
- (9) Knijnenburg, Q.; Hettterscheid, D.; Kooistra, T. M.; Budzelaar, P. H. M. *Eur. J. Inorg. Chem.* **2004**, 1204.
- (10) (a) Kahn, O. *Molecular Magnetism*; Wiley-VCH: New York, 1993. (b) Kanamori, J. J. *Phys. Chem. Solids* **1959**, *10*, 87. (c) Goodenough, J. B. *J. Phys. Chem. Solids* **1958**, *6*, 287. (d) Goodenough, J. B. *Phys. Rev.* **1955**, *100*, 564.
- (11) Danopoulos, A. A.; Wright, J. A.; Motherwell, W. B. *Chem. Commun.* **2005**, 784.

- (12) Bart, S. C.; Lobkovsky, E.; Chirik, P. J. *J. Am. Chem. Soc.* **2004**, *126*, 13794.
- (13) Bouwkamp, M. W.; Bowman, A. W.; Lobkovsky, E.; Chirik, P. J. *J. Am. Chem. Soc.* **2006**, *128*, 13340.
- (14) Campora, J.; Palma, P.; Carmona, E. *Coord. Chem. Rev.* **1999**, *193–95*, 207.
- (15) Mehn, M. P.; Peters, J. C. *J. Inorg. Biochem.* **2006**, *100*, 634.
- (16) Bart, S. C.; Lobkovsky, E.; Bill, E.; Chirik, P. J. *J. Am. Chem. Soc.* **2006**, *128*, 5302.
- (17) Bart, S. C.; Bowman, A. C.; Lobkovsky, E.; Chirik, P. J. *J. Am. Chem. Soc.* **2007**, *129*, 7212.

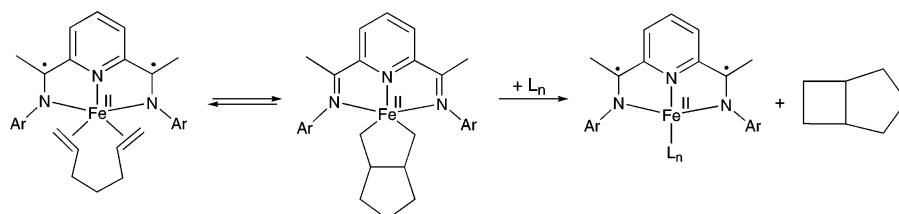


Figure 3. Catalytic  $[2\pi + 2\pi]$  cycloaddition promoted by bis(imino)pyridine iron.

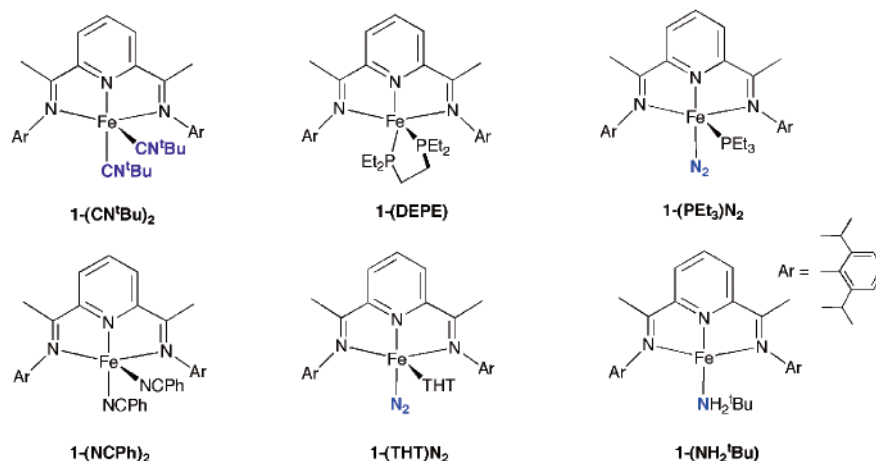


Figure 4. Bis(imino)pyridine iron neutral-ligand compounds prepared in this study.

ate donor to yield the desired neutral-ligand derivative. As will be described below, coordination of either one or two new donors was observed and, in some cases, retention of one of the  $N_2$  ligands occurred.

Addition of 2 equiv of *tert*-butyl isonitrile to **1-(N<sub>2</sub>)<sub>2</sub>** furnished purple crystals identified as the five-coordinate, diamagnetic bis(isonitrile) complex,  $(^{iPr}PDI)Fe(CN^tBu)_2$  (**1-(CN<sup>t</sup>Bu)<sub>2</sub>**) (Figure 4). The benzene-*d*<sub>6</sub> <sup>1</sup>H NMR spectrum of **1-(CN<sup>t</sup>Bu)<sub>2</sub>** at 23 °C exhibits the number of peaks for a *C*<sub>s</sub>-symmetric molecule with distinct resonances for the *tert*-butyl groups for the inequivalent apical and basal positions. Accordingly, four inequivalent isopropyl methyl and two methine groups on the bis(imino)pyridine chelate are also observed. This behavior is in contrast to other five-coordinate complexes, **1-(CO)<sub>2</sub>** and **1-(N<sub>2</sub>)<sub>2</sub>**, where rapid exchange between the apical and basal positions occurs on the NMR time scale. The observation of distinct apical and basal sites of **1-(CN<sup>t</sup>Bu)<sub>2</sub>** is likely a consequence of the large *tert*-butyl groups which raise the barrier for site interchange. Notably, all of the <sup>1</sup>H NMR resonances appear close to their diamagnetic reference values, establishing little to no contribution from paramagnetic excited states.

Treatment of **1-(N<sub>2</sub>)<sub>2</sub>** with a stoichiometric quantity of the bis(phosphine), Et<sub>2</sub>PCH<sub>2</sub>CH<sub>2</sub>PEt<sub>2</sub> (DEPE), furnished black crystals identified as  $(^{iPr}PDI)Fe(DEPE)$  (**1-DEPE**) (Figure 4). As with **1-(CN<sup>t</sup>Bu)<sub>2</sub>**, the benzene-*d*<sub>6</sub> <sup>1</sup>H NMR spectrum of **1-DEPE** recorded at 23 °C exhibits the number of peaks for a *C*<sub>s</sub>-symmetric compound with unique apical and basal phosphine coordination sites, indicating slow site exchange on the NMR time scale. Inequivalent protons are observed by <sup>1</sup>H NMR spectroscopy for the methylene groups of the backbone of the DEPE ligand. Accordingly, the <sup>31</sup>P{<sup>1</sup>H} NMR spectrum exhibits two peaks centered at −45.46 and

77.01 ppm for the inequivalent phosphines. Again, each of the  $[^{iPr}PDI]$  resonances appear close to their diamagnetic reference values, demonstrating a pure *S* = 0 ground state with little contribution from *S* = 1 excited states.

Addition of 1 equiv of monodentate  $\sigma$ -donors to **1-(N<sub>2</sub>)<sub>2</sub>** resulted in five-coordinate complexes where one of the  $N_2$  ligands is retained. For example, treatment of **1-(N<sub>2</sub>)<sub>2</sub>** with 1 equiv of PEt<sub>3</sub> produced a bright green solid identified as  $(^{iPr}PDI)Fe(PEt_3)N_2$  (**1-(PEt<sub>3</sub>)N<sub>2</sub>**). Coordinated dinitrogen was confirmed by X-ray diffraction (vide infra), infrared spectroscopy, and <sup>15</sup>N NMR studies. A strong N≡N stretch centered at 2028 cm<sup>−1</sup> was observed in the KBr infrared spectrum and shifted slightly to 2051 cm<sup>−1</sup> upon dissolution in pentane. Additionally, two <sup>15</sup>N NMR resonances were observed at 330.23 and 354.43 ppm for the inequivalent nitrogen atoms of the  $N_2$  ligand.

Danopoulos and co-workers<sup>11</sup> have reported the synthesis and characterization of related pyridine bis(*N*-heterocyclic carbene) iron phosphine dinitrogen complexes with PMe<sub>3</sub> and PCy<sub>3</sub>. Both compounds are diamagnetic with no NMR spectroscopic evidence for contributions from paramagnetic excited states. The PMe<sub>3</sub> compound exhibits an N≡N stretch at 2032 cm<sup>−1</sup> in Nujol, similar to the value obtained in the solid state for **1-(PEt<sub>3</sub>)N<sub>2</sub>**.

The ambient temperature <sup>1</sup>H NMR spectrum of **1-(PEt<sub>3</sub>)N<sub>2</sub>** in toluene-*d*<sub>8</sub> exhibits five broadened peaks in the diamagnetic region, suggesting a dynamic process on the NMR time scale. Cooling the solution (Figure 5) resulted in a gradual sharpening of the peaks as a function of temperature. At −80 °C, the number of peaks expected for a *C*<sub>s</sub>-symmetric compound was observed. The dynamic process is most likely dissociation and recoordination of either the dinitrogen or the PEt<sub>3</sub> ligand on the NMR time scale.

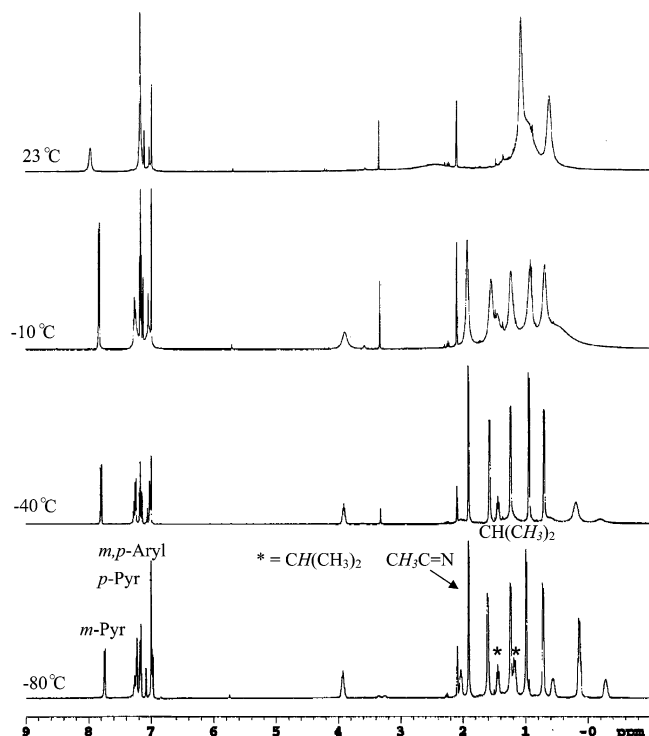


**Figure 5.** Variable-temperature  $^1\text{H}$  NMR spectra of  $1-(\text{PEt}_3)\text{N}_2$  in toluene- $d_8$ .

Importantly, all of the resonances appear close to their diamagnetic reference values, suggesting little or no contribution from TIP.

Addition of a sulfur rather than phosphorus donor changes the  $^1\text{H}$  NMR spectroscopic properties of the resulting iron compound dramatically. The tetrahydrothiophene (THT) complex,  $1-(\text{THT})\text{N}_2$ , was isolated as a brown-red powder following addition of 1 equiv of THT to  $1-(\text{N}_2)_2$  and recrystallization from pentane at  $-35^\circ\text{C}$ . Confirmation of the dinitrogen ligand was provided by infrared spectroscopy. An intense  $\text{N}\equiv\text{N}$  band was identified at  $2045\text{ cm}^{-1}$  in the solid-state (KBr) spectrum, a slightly higher frequency than that for  $1-(\text{PEt}_3)\text{N}_2$  ( $\nu_{\text{N}_2} = 2028\text{ cm}^{-1}$ ). This observation is likely a consequence of THT being a weaker-field ligand than  $\text{PEt}_3$ .

The benzene- $d_6$   $^1\text{H}$  NMR spectrum of  $1-(\text{THT})\text{N}_2$  recorded at  $23^\circ\text{C}$  exhibits the number of peaks expected for a molecule of  $C_{2v}$  symmetry, suggesting a rapid dynamic process, most likely  $\text{N}_2$  or THT dissociation and recoordination, on the NMR time scale. Such a process renders equivalent the aryl substituents above and below the iron chelate plane. Notably, the in-plane hydrogens on the [ $^i\text{PrPDI}$ ] chelate are shifted from their diamagnetic reference values. The imine methyl group,  $\text{N}=\text{CMe}$ , appears as a singlet centered at  $-4.62\text{ ppm}$ , significantly upfield of the shift observed at  $2.08\text{ ppm}$  for  $1-(\text{CO})_2$  and  $2.31\text{ ppm}$  for  $1-(\text{CN}^i\text{Bu})_2$ . Both the *p*- and *m*-pyridine hydrogens are shifted downfield to  $9.14$  and  $10.97\text{ ppm}$ , respectively, from free  $^i\text{PrPDI}$ . Chemical shifts with this dispersion are indicative of TIP,<sup>6</sup> suggesting that coordination of weaker,  $\sigma$ -type ligands results in a more energetically accessible  $S = 1$  excited state.<sup>6</sup> Importantly, no change in chemical shifts was

observed upon cooling the sample to  $-80^\circ\text{C}$ , as would be expected for a temperature-dependent paramagnet obeying the Curie–Weiss Law.

The amine complex,  $1-(\text{NH}_2^i\text{Bu})$ , was prepared by addition of *tert*-butylamine to  $1-(\text{N}_2)_2$  and was isolated as a brown solid. Integration of the benzene- $d_6$   $^1\text{H}$  NMR spectrum established coordination of only 1 equiv of amine. Both infrared spectroscopy and combustion analysis are also consistent with a four-coordinate iron compound without a dinitrogen ligand. Evidence for an intact amine ligand, rather than an  $\text{N}-\text{H}$  oxidative addition product, is derived from observation of a broad peak centered at  $5.55\text{ ppm}$  integrating to two protons ( $^1\text{H}$  NMR) and an  $\text{N}-\text{H}$  stretch centered at  $3322\text{ cm}^{-1}$  in the solid-state (KBr) infrared spectrum. The  $^1\text{H}$  NMR chemical shifts of the in-plane hydrogens indicate TIP.<sup>7</sup> An upfield-shifted imine methyl group,  $\text{N}=\text{CMe}$ , is observed at  $-7.02\text{ ppm}$ , while the *p*- and *m*-pyridine peaks appear downfield at  $8.87$  and  $11.50\text{ ppm}$ , respectively. As shown in Figure 6, these peaks do not shift upon cooling a toluene- $d_8$  solution to  $-80^\circ\text{C}$ . The broadening observed at  $-10^\circ\text{C}$  is likely due to exchange between free and coordinated amine on the NMR time scale.

One final compound,  $1-(\text{NCPh})_2$ , was prepared by addition of 2 equiv of benzonitrile to  $1-(\text{N}_2)_2$ . This compound exhibits spectroscopic features between the pure  $S = 0$  compounds (e.g.,  $1-(\text{CN}^i\text{Bu})_2$ ,  $1-\text{DEPE}$ ) and those that have contributions from  $S = 1$  excited states. The imine methyl resonance is shifted to  $0.09\text{ ppm}$ , upfield of the diamagnetic reference value of  $2.27\text{ ppm}$  for free  $^i\text{PrPDI}$ . However, this deviation is much smaller than those observed with  $1-\text{DMAP}$  or  $1-(\text{NH}_2^i\text{Bu})$ , suggesting a diminished contribution from  $S = 1$  excited states upon introduction of the modest  $\pi$ -acceptor.

Compiled in Table 1 are the  $^1\text{H}$  NMR chemical shifts ( $23^\circ\text{C}$ ) of the in-plane bis(imino)pyridine chelate hydrogens for each iron derivative recorded in benzene- $d_6$ . The absolute value of the difference in the imine methyl group chemical shift of the compound of interest and that in the free  $^i\text{PrPDI}$  ligand provides a measure of the contribution from paramagnetic excited states. For complexes with the strongest field ligands in the series,  $1-(\text{CO})_2$  and  $1-(\text{CN}^i\text{Bu})_2$ , this difference is near zero and indicates no detectable contribution from TIP. Slightly reducing the field strength to phosphine ligands slightly increases the chemical shift difference.

At the other extreme are compounds bearing relatively weak-field, purely  $\sigma$ -donating amines<sup>18</sup> such as  $1-(\text{NH}_2^i\text{Bu})$  and  $1-(\text{NHC}_6\text{H}_{10})$ , which exhibit the largest chemical-shift displacements in the series corresponding to the largest contributions from TIP. As was observed with  $1-\text{DMAP}$ ,<sup>6</sup> the diamagnetic ground state of each iron compound establishes that the lowest energy state is the  $S_{\text{Fe}} = 1$  ferrous ion and is antiferromagnetically coupled to the triplet ( $S_{\text{L}} = 1$ ) [ $\text{PDI}$ ] $^{2-}$  anion. Contribution from the low-lying excited state, where the bis(imino)pyridine ligand is a spin singlet

(18) Leyssens, T.; Peeters, D.; Orpen, A. G.; Harvey, J. N. *Organometallics* **2007**, *26*, 2637.



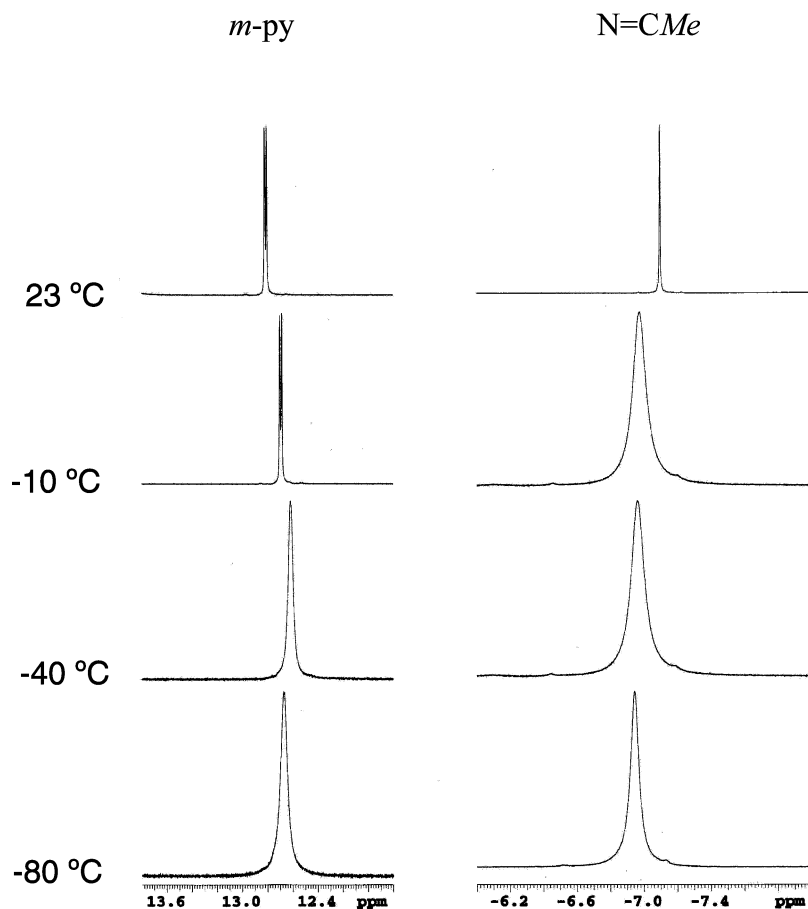


**Figure 6.** Variable-temperature  $^1\text{H}$  NMR spectra of **1**-( $\text{NH}_2^t\text{Bu}$ ) in toluene- $d_8$  highlighting the *m*-pyridine and imine methyl resonances.

**Chart 1**

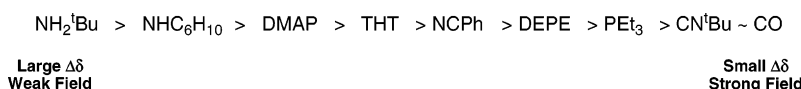


**Table 1.**  $^1\text{H}$  NMR Chemical Shifts of the In-Plane Bis(imino)pyridine Hydrogens for Spectra Recorded in Benzene- $d_6$  at 23  $^\circ\text{C}$

compound	$\delta$ N=CMe (ppm)	$\delta$ <i>m</i> -pyridine (ppm)	$\delta$ <i>p</i> -pyridine (ppm)	$ \Delta\delta $ (ppm) <sup>c</sup>
<b>iPrPDI</b>	2.27	8.50	7.28	0
<b>1-(CN<sup>t</sup>Bu)<sub>2</sub></b>	2.31	7.11	7.20	0.04
<b>1-(CO)<sub>2</sub></b> <sup>a</sup>	2.08	7.63	7.20	0.19
<b>1-(PET<sub>3</sub>)N<sub>2</sub></b>	1.90	7.75	7.28	0.37
<b>1-(DEPE)</b>	1.71	8.27	7.39	0.56
<b>1-(NCPH)<sub>2</sub></b>	0.09	10.83	8.87	2.18
<b>1-(THT)N<sub>2</sub></b>	-4.62	10.97	9.14	6.89
<b>1-DMAP</b> <sup>a</sup>	-5.85	12.42	7.04	8.12
<b>1-(NH<sub>2</sub><sup>t</sup>Bu)</b>	-7.02	11.50	8.87	9.29
<b>1-(NHC<sub>6</sub>H<sub>10</sub>)</b> <sup>b</sup>	-6.90	12.89	8.87	9.17

<sup>a</sup> Data taken from ref 6. <sup>b</sup> Data taken from ref 12. <sup>c</sup> Difference in chemical shift between the imine methyl group in the compound of interest and the free **iPrPDI** ligand.

( $S_L = 0$ ), is the origin of TIP and the unusual  $^1\text{H}$  NMR chemical shifts. Introduction of a ligand of intermediate field strength, benzonitrile, resulted in a chemical shift dispersion between the two extremes with an N=CMe group appearing at 0.09 ppm. Chart 1 ranks the chemical shift dispersion observed in the bis(imino)pyridine iron complexes as a function of ligand.

**Solid-State Structures.** Four compounds reported in this study were characterized by X-ray diffraction. The molecular

structures of **1-(CN<sup>t</sup>Bu)<sub>2</sub>** and **1-DEPE** are presented in Figure 7, while those of **1-(PET<sub>3</sub>)N<sub>2</sub>** and **1-(THT)N<sub>2</sub>** are shown in Figure 8. The overall molecular geometry of each compound is best described as distorted square pyramidal where the bis(imino)pyridine chelate defines the three sites of the idealized basal plane. For both **1-(PET<sub>3</sub>)N<sub>2</sub>** and **1-(THT)N<sub>2</sub>**, the more  $\pi$ -acidic dinitrogen ligand occupies the basal position while the  $\sigma$ -ligand is coordinated in the apical site. **1-(PET<sub>3</sub>)N<sub>2</sub>** is structurally similar to a related pyridine bis-(*N*-heterocyclic carbene) iron trimethylphosphine dinitrogen compound reported by Danopoulos.<sup>11</sup>

The metrical parameters for the bis(imino)pyridine chelates of the iron derivatives are presented in Table 2. Data for the free ligand, as well as other compounds crystallographically characterized in our laboratory,<sup>6,12,13</sup> are also reported for comparison. All of the iron compounds presented in Table 2 exhibit elongated  $\text{C}_{\text{imine}}\text{--N}_{\text{imine}}$  and  $\text{C}_{\text{ipso}}\text{--N}_{\text{pyridine}}$  bonds in addition to contracted  $\text{C}_{\text{imine}}\text{--C}_{\text{ipso}}$  bonds with respect to free **iPrPDI**, consistent with two-electron reduction of the chelate to form  $[\text{iPrPDI}]^{2-}$ .<sup>6</sup> The two new dinitrogen complexes, **1-(PET<sub>3</sub>)N<sub>2</sub>** and **1-(THT)N<sub>2</sub>**, have short N–N bonds of 1.0853(16) and 1.117(3) Å, indicating little reduction by the ferrous center.

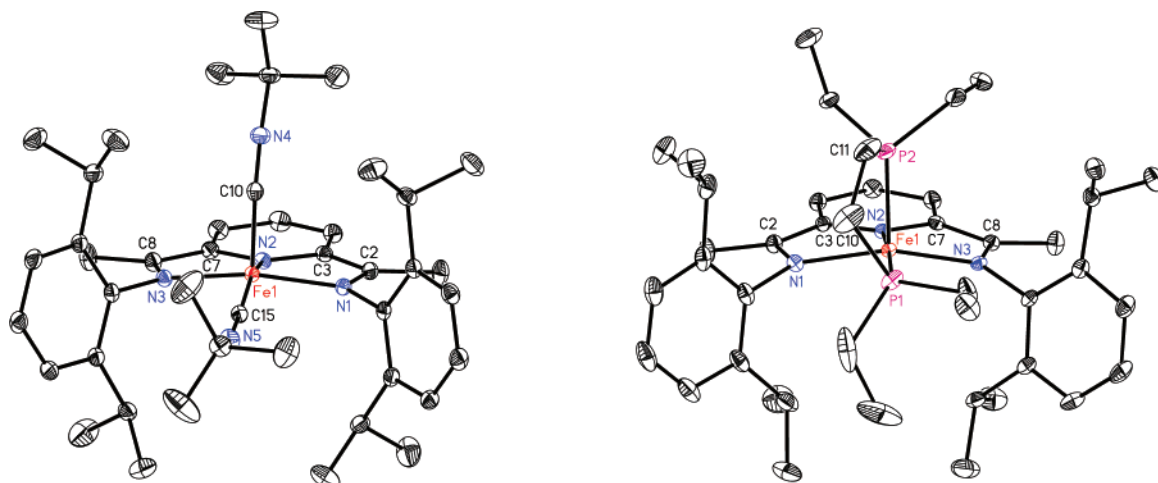


Figure 7. Molecular structures of **1-(CN<sup>t</sup>Bu)<sub>2</sub>** and **1-DEPE** at 30% probability ellipsoids. Hydrogen atoms omitted for clarity.

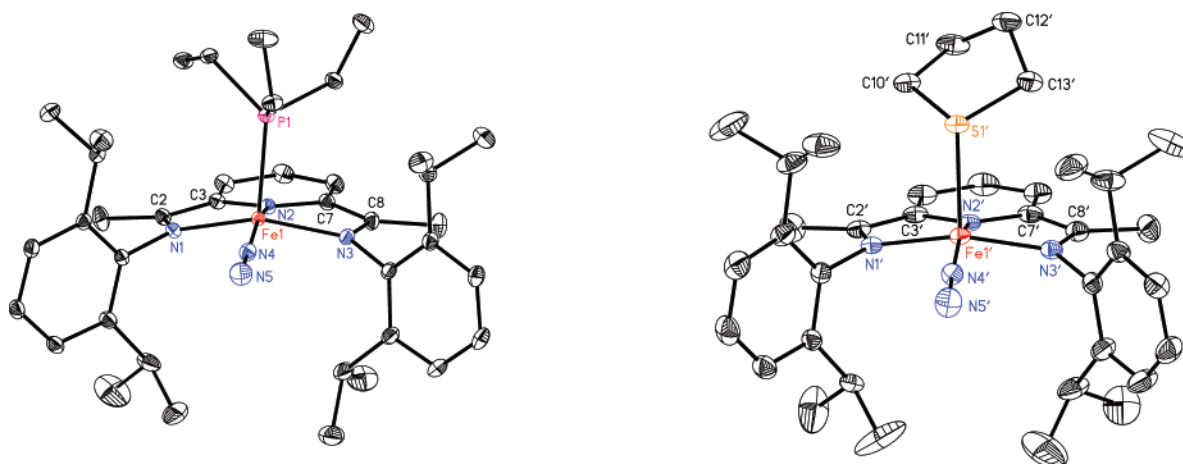


Figure 8. Molecular structures of **1-(PET<sub>3</sub>)N<sub>2</sub>** and **1-(THT)N<sub>2</sub>** at 30% probability ellipsoids. Hydrogen atoms omitted for clarity.

Table 2. Selected Bond Distances (Å) for Crystallographically Characterized Bis(imino)pyridine Chelates

compound	N <sub>imine</sub> –C <sub>imine</sub>	C <sub>imine</sub> –C <sub>ipso</sub>	C <sub>ipso</sub> –N <sub>pyridine</sub>
iPr <sup>+</sup> PDI <sup>a</sup>	1.274(3)	1.489(3)	1.342(3)
	1.274(3)	1.487(3)	1.345(3)
<b>1-(CN<sup>t</sup>Bu)<sub>2</sub></b>	1.3408(16)	1.4177(19)	1.3844(16)
	1.3370(17)	1.4220(18)	1.3788(17)
<b>1-(CO)<sub>2</sub></b> <sup>a</sup>	1.330(2)	1.425(2)	1.376(2)
	1.335(5)	1.423(2)	1.372(2)
<b>1-(N<sub>2</sub>)<sub>2</sub></b> <sup>b</sup>	1.333(2)	1.427(2)	1.376(2)
	1.332(2)	1.428(3)	1.379(2)
<b>1-DEPE</b>	1.351(3)	1.412(3)	1.376(3)
	1.358(3)	1.405(3)	1.380(3)
<b>1-(PET<sub>3</sub>)N<sub>2</sub></b>	1.3533(16)	1.4167(17)	1.3750(15)
	1.3471(14)	1.4147(17)	1.3749(15)
<b>1-(THT)N<sub>2</sub></b>	1.335(3)	1.431(4)	1.379(3)
	1.352(3)	1.428(3)	1.372(3)
<b>1-DMAP</b> <sup>a</sup>	1.358(5)	1.405(5)	1.387(5)
	1.350(5)	1.414(5)	1.389(5)
<b>1-(HNC<sub>6</sub>H<sub>10</sub>)</b> <sup>c</sup>	1.360(5)	1.412(6)	1.360(5)
	1.372(5)	1.389(6)	1.386(5)

<sup>a</sup> Data taken from ref 6. <sup>b</sup> Data taken from ref 12. <sup>c</sup> Data taken from ref 13.

While distortions within the series are relatively small, a general trend in the structural data may be established, where better  $\sigma$ -donors produce the most electron-rich iron center and hence the greatest backbonding into the bis(imino)pyridine chelate. Relatively large chelate distortions, par-

ticularly in the C<sub>imine</sub>–C<sub>ipso</sub> distances, are observed in **1-DEPE** and **1-(PET<sub>3</sub>)N<sub>2</sub>**, and are likely a consequence of the strong  $\sigma$ -donation of the phosphines which in turn engenders an electron-rich iron center capable of engaging in electron transfer with the bis(imino)pyridine. Accordingly, complexes bearing the nitrogen donors, **1-DMAP** and **1-(NHC<sub>6</sub>H<sub>10</sub>)**, exhibit similar distortions. Compounds containing  $\pi$ -acids, **1-(CO)<sub>2</sub>**, **1-(CN<sup>t</sup>Bu)<sub>2</sub>**, and **1-(N<sub>2</sub>)<sub>2</sub>**, have the smallest distortions in the series. Notably, the metrical parameters of **1-(CO)<sub>2</sub>** and **1-(CN<sup>t</sup>Bu)<sub>2</sub>** are statistically indistinguishable from those for **1-(N<sub>2</sub>)<sub>2</sub>**, despite the difference in electronic structure. This observation demonstrates that the spin state of the ligand has little influence on the metrical parameters, as predicted by DFT calculations.<sup>6</sup>

**Mössbauer Spectroscopy.** Although X-ray diffraction has proven effective for identifying bis(imino)pyridine chelate reduction, no statistical difference in bond lengths was observed between pure  $S = 0$  compounds and those exhibiting TIP.<sup>6</sup> In contrast, NMR spectroscopy does differentiate the compounds by virtue of the chemical shift dispersion of the in-plane chelate hydrogens. Zero-field Mössbauer spectroscopy was performed at 80 K to further explore and distinguish the electronic structure of the compounds as a function of neutral donor.

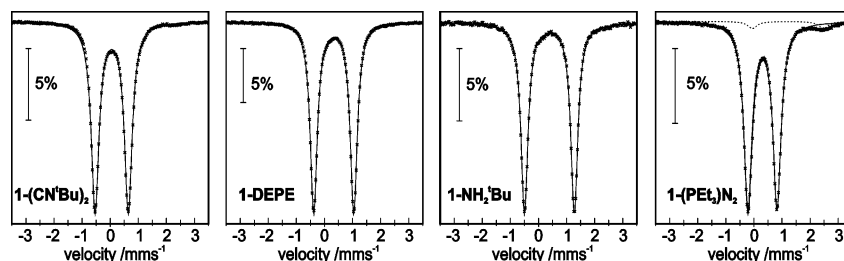


**Figure 9.** Zero-field Mössbauer spectra for **1-(CN<sup>t</sup>Bu)<sub>2</sub>** (left), **1-DEPE** (center left), **1-(NH<sub>2</sub><sup>t</sup>Bu)** (center right), and **1-(PEt<sub>3</sub>)N<sub>2</sub>** (right) recorded at 80 K. The ordinate shows relative transmission, and the solid lines are the result of fits by using Lorentzian doublets. The dotted line in the right panel is a minor contribution from an iron(II) or iron(III) high-spin contaminant accounting for 4% of the observed iron, with  $\delta = 1.21$  mm/s and  $\Delta E_Q = 2.53$  mm/s.

**Table 3.** Zero-Field Mössbauer Parameters for a Family of Bis(imino)pyridine Iron Neutral-Ligand Derivatives

compound	$\delta$ (mm/s)	$\Delta E_Q$ (mm/s)	%
<b>1-(CN<sup>t</sup>Bu)<sub>2</sub></b>	0.06	1.18	100
<b>1-(CO)<sub>2</sub></b>	0.03	1.17	ref 6
<b>1-(N<sub>2</sub>)<sub>2</sub></b>	0.39	0.53	ref 6
<b>1-N<sub>2</sub></b>	0.38	1.76	ref 6
<b>1-(DEPE)</b>	0.33	1.43	100
<b>1-(PEt<sub>3</sub>)N<sub>2</sub></b>	0.30	1.04	96
	1.21	2.53	4
<b>1-(NH<sub>2</sub><sup>t</sup>Bu)</b>	0.39	1.78	100
<b>1-DMAP</b>	0.31	1.94	ref 6

Representative spectra for **1-(CN<sup>t</sup>Bu)<sub>2</sub>**, **1-(DEPE)**, and **1-(NH<sub>2</sub><sup>t</sup>Bu)** are presented in Figure 9. The resulting isomer shifts ( $\delta$ ) and quadrupole splittings ( $\Delta E_Q$ ) are reported in Table 3. Also included in Table 3 are the values for **1-(CO)<sub>2</sub>**, **1-DMAP**, **1-(N<sub>2</sub>)<sub>2</sub>**, and **1-(N<sub>2</sub>)** for comparison.<sup>6</sup> The experimental isomer shifts demonstrate that the Mössbauer parameters are sensitive to the field strength of the neutral donor. In general, two classes of compounds have been identified.

The first are those with isomer shifts around 0 mm/s. These compounds have  $\pi$ -acids and pure  $S = 0$  ground states, as judged by <sup>1</sup>H NMR spectroscopy. The isomer shifts of 0.03 and 0.06 mm/s for **1-(CO)<sub>2</sub>** and **1-(CN<sup>t</sup>Bu)<sub>2</sub>**, respectively, are consistent with low-spin iron(II) and are similar to the archetypal low-spin iron(II) dication, [Fe(CO)<sub>6</sub>]<sup>2+</sup> with  $\delta = 0$  mm/s.<sup>19</sup> Covalency and backbonding may yield some contribution from an iron(0) canonical form as established by previously reported DFT calculations.<sup>6,12</sup>

The second class of compounds have isomer shifts in the range of 0.30–0.40 mm/s. Specific examples include the mono- and bis(dinitrogen) complexes **1-N<sub>2</sub>** and **1-(N<sub>2</sub>)<sub>2</sub>** with isomer shifts of 0.38 and 0.39 mm/s, as well as complexes bearing weaker-field ligands such as **1-(NH<sub>2</sub><sup>t</sup>Bu)** with a  $\delta$  value of 0.39 mm/s. Values in this range are consistent with an intermediate-spin iron center ( $S_{Fe} = 1$ ) with a doubly reduced bis(imino)pyridine chelate. These compounds, along with **1-DMAP**, **1-DEPE**, and **1-(PEt<sub>3</sub>)N<sub>2</sub>**, are more classical Werner-type compounds as compared to **1-(CO)<sub>2</sub>** and **1-(CN<sup>t</sup>Bu)<sub>2</sub>** and as a consequence have a lower degree of covalency. Notably, all of these compounds have isomer shifts lower than those reported for **1-Cl** and **1-Cl<sub>2</sub>**,<sup>6</sup> supporting a higher degree of chelate reduction for the neutral-ligand derivatives.

The Mössbauer spectrum for **1-(PEt<sub>3</sub>)N<sub>2</sub>** (Figure 9) deserves additional comment. Recording the data at zero-field at 80 K reveals a major compound accounting for 96% of the iron with the expected 0.30 mm/s isomer shift. A minor compound, accounting for 4% of the observed iron, was also observed with  $\delta = 1.21$  mm/s and  $\Delta E_Q = 2.53$  mm/s, consistent with a high-spin iron(II) or iron(III) compound. Regardless, the spectroscopic parameters for **1-(PEt<sub>3</sub>)N<sub>2</sub>** clearly establish an intermediate-spin ferrous ion with a dianionic bis(imino)pyridine chelate.

Thus, Mössbauer spectroscopy has proven useful in differentiating the spin state of the iron center of the various neutral-ligand derivatives of bis(imino)pyridine iron. The compounds bearing the strongest field ligands are low-spin iron(II) with isomer shifts around 0 mm/s. Those with weaker-field ligands have higher isomer shifts consistent with intermediate-spin iron centers and reduced covalency, indicative of more classical coordination compounds. However, Mössbauer spectroscopy is ineffective in distinguishing contributions from TIP within this series of molecules.

## Concluding Remarks

In summary, a family of neutral-ligand derivatives of bis(imino)pyridine iron have been prepared and in many cases characterized by X-ray diffraction and Mössbauer spectroscopy. In each example, the metrical parameters determined by X-ray crystallography establish a doubly reduced bis(imino)pyridine chelate. The combination of Mössbauer isomer shift and <sup>1</sup>H NMR chemical shifts of the in-plane hydrogens of the chelate provide further information about the electronic structure of the compounds. For those with the strongest field ligands in the series, carbon monoxide and *tert*-butylisocyanide, the Mössbauer isomer shift establishes low-spin iron(II) centers while <sup>1</sup>H NMR spectroscopy demonstrates little contribution from TIP. As the field strength of the ligand is reduced to principally  $\sigma$ -donors, the Mössbauer isomer shift increases, consistent with intermediate-spin iron(II). Within this spin state, <sup>1</sup>H NMR spectroscopy is particularly valuable for identifying contributions from paramagnetic excited states arising from an  $S = 0$  form of the chelate. In the case of strong  $\sigma$ -donors, these contributions are minimal, as evidenced by the relatively small chemical shift dispersions of the imine methyl and pyridine hydrogens. In the case of weaker-field amine and sulfur donors, the contributions from the paramagnetic excited states increase and the chemical shift dispersion increases accordingly.

(19) Bernhardt, E.; Bley, B.; Wartchow, R.; Willner, H.; Bill, E.; Kuhn, P.; Sham, I. H. T.; Bodenbinder, M.; Brochler, R.; Aubke, F. *J. Am. Chem. Soc.* **1999**, *121*, 7188.

Overall, this work demonstrates that the spin state of the ligand and hence contributions from paramagnetic excited states can be readily manipulated by judicious choice of ligand within the spectrochemical series.

## Experimental Section

**General Considerations.** All air- and moisture-sensitive manipulations were carried out using standard vacuum line, Schlenk, and cannula techniques or in an MBraun inert-atmosphere dry box containing an atmosphere of purified nitrogen. The dry box was equipped with a cold well designed for freezing samples in liquid nitrogen. Solvents for air- and moisture-sensitive manipulations were initially dried and deoxygenated using literature procedures.<sup>20</sup> Argon and hydrogen gas were purchased from Airgas Incorporated and passed through a column containing manganese oxide supported on vermiculite and 4 Å molecular sieves before admission to the high-vacuum line. Benzene-*d*<sub>6</sub> was purchased from Cambridge Isotope Laboratories and distilled from sodium metal under an atmosphere of argon and stored over 4 Å molecular sieves and sodium metal. Benzonitrile, *tert*-butylamine, triethylphosphine, and diethylphosphinoethane were dried over molecular sieves. Tetrahydrothiophene and *tert*-butylisocyanide were dried over calcium hydride and vacuum-transferred before use. **1-(N<sub>2</sub>)<sub>2</sub>**, **1-DMAP**, and **1-(CO)<sub>2</sub>** were prepared according to literature procedures.<sup>6,12</sup>

<sup>1</sup>H NMR spectra were recorded on Varian Mercury 300 and Inova 400 and 500 spectrometers operating at 299.763, 399.780, and 500.62 MHz, respectively. All chemical shifts are reported relative to SiMe<sub>4</sub> using <sup>1</sup>H (residual) chemical shifts of the solvent as a secondary standard. <sup>15</sup>N NMR spectra were recorded on a Varian Inova 500 spectrometer operating at 50.663 MHz, and chemical shifts were externally referenced to liquid ammonia. <sup>31</sup>P-{<sup>1</sup>H} NMR chemical shifts are reported downfield from H<sub>3</sub>PO<sub>4</sub> and referenced to an external 85% H<sub>3</sub>PO<sub>4</sub> solution. Elemental analyses were performed at Robertson Microlit Laboratories, Inc., Madison, NJ. Single crystals suitable for X-ray diffraction were coated with polyisobutylene oil in a drybox, transferred to a nylon loop, and then quickly transferred to the goniometer head of a Bruker X8 APEX2 diffractometer equipped with a molybdenum X-ray tube ( $\lambda = 0.71073$  Å). Preliminary data revealed the crystal system. A hemisphere routine was used for data collection and determination of lattice constants. The space group was identified and the data were processed using the Bruker SAINT+ program and corrected for absorption using SADABS. The structures were solved using direct methods (SHELXS) completed by subsequent Fourier synthesis and refined by full-matrix least-squares procedures. Infrared data were collected either in the solid state (KBr pellet) or in pentane solution.

Mössbauer data were collected on an alternating constant-acceleration spectrometer. The minimum experimental line width was 0.24 mm/s (full width at half-height). A constant sample temperature was maintained with an Oxford Instruments Variox or an Oxford Instruments Mössbauer-Spectromag 2000 cryostat. Reported isomer shifts ( $\delta$ ) are referenced to iron metal at 293 K.

**Preparation of (i<sup>Pr</sup>PDI)Fe(CN<sup>t</sup>Bu)<sub>2</sub> (1-(CN<sup>t</sup>Bu)<sub>2</sub>).** A 50-mL round-bottomed flask was charged with 0.115 g (0.194 mmol) **1-(N<sub>2</sub>)<sub>2</sub>** and ~20 mL of pentane. The flask was fitted with a 180° needle valve, removed from the glovebox, and placed in a -78 °C bath. On the high-vacuum line, the flask was degassed. Using a calibrated gas bulb, 2 equiv of *tert*-butylisocyanide were added to the flask, immediately producing a color change from olive green

**Table 4.** UV-Visible Data for a Family of Bis(imino)pyridine Iron Neutral-Ligand Compounds

compound	$\lambda$ (nm)	$\epsilon$ (M <sup>-1</sup> cm <sup>-1</sup> )
<b>1-N<sub>2</sub></b>	444	7500
	544	1922
	700.5	2680
	910	848
	1206	453
	337	5062
	480	4610
<b>1-DMAP</b>	577	1956
	667.5	521
	1067	660
<b>1-PET<sub>3</sub>(N<sub>2</sub>)</b>	448	9223
	651	3421
<b>1-(CN<sup>t</sup>Bu)<sub>2</sub></b>	985.5	1570
	409	5575
	534	3461
	918	1871
<b>1-DEPE</b>	448.5	8812
	708.5	5057
	1292	1347
	470	9375
	550	3229
<b>1-(THT)(N<sub>2</sub>)</b>	656	1477
	765	1154
	1088	1033
	284	14797
	344	11340
	458	5880
<b>1-(NH<sub>2</sub><sup>t</sup>Bu)</b>	568	1962
	730	1015
	1040	1182

to purple. The resulting reaction mixture was warmed to ambient temperature and stirred for 1 h. The volatile components were removed in vacuo to yield 0.134 g (98%) of a purple solid identified as **1-(CN<sup>t</sup>Bu)<sub>2</sub>**. Anal. Calcd for C<sub>43</sub>H<sub>61</sub>N<sub>5</sub>Fe: C, 73.38; H, 8.74; N, 9.95. Found C, 72.97; H, 8.98; N, 9.60. <sup>1</sup>H NMR (benzene-*d*<sub>6</sub>):  $\delta$  0.53 (s, 9H, C(CH<sub>3</sub>)<sub>3</sub>), 0.80 (s, 9H, C(CH<sub>3</sub>)<sub>3</sub>), 0.90 (d, 6.2 Hz, 6H, CHMe<sub>2</sub>), 1.01 (d, 6.2 Hz, 6H, CHMe<sub>2</sub>), 1.34 (d, 6.6 Hz, 6H, CHMe<sub>2</sub>), 1.63 (d, 5.9 Hz, 6H, CHMe<sub>2</sub>), 2.23 (q, 6.0 Hz, 2H, CHMe<sub>2</sub>), 2.31 (s, 6H, C(Me)), 3.26 (q, 7.0 Hz, 2H, CHMe<sub>2</sub>), 7.11 (d, 7.3 Hz, 2H, *m*-pyridine or *p*-aryl), 7.19–7.29 (m, 5H, *p*-pyridine and *m*-aryl), 8.01 (d, 7.4 Hz, 2H, *m*-pyridine or *p*-aryl). <sup>13</sup>C NMR (benzene-*d*<sub>6</sub>):  $\delta$  16.23 (C(Me)), 23.84 (CHMe<sub>2</sub>), 24.67 (CHMe<sub>2</sub>), 26.74 (CHMe<sub>2</sub>), 27.49 (CHMe<sub>2</sub>), 28.65 (CHMe<sub>2</sub>), 31.01 (CMe<sub>3</sub>), 115.00 (*p*-pyridine), 116.71 (*m*-pyridine or *p*-aryl), 123.03 (*m*-aryl, *m*-pyridine or *p*-aryl), 124.62 (*m*-aryl, *m*-pyridine or *p*-aryl), 139.82, 142.04, 145.38, 148.77, 153.24. IR (KBr):  $\nu_{\text{CN}}$  = 1976, 2056 cm<sup>-1</sup>.

**Preparation of (i<sup>Pr</sup>PDI)Fe(Et<sub>2</sub>PCH<sub>2</sub>CH<sub>2</sub>PEt<sub>2</sub>) (1-DEPE).** A 20-mL scintillation vial was charged with 0.057 g (0.096 mmol) **1-(N<sub>2</sub>)<sub>2</sub>** and ~5 mL of pentane. To the vial was added 0.022 mL (0.096 mmol) of diethylphosphinoethane by microsyringe with stirring. The addition resulted in an immediate color change from olive green to red-brown. After the reaction mixture was stirred for 1 h, all of the volatiles were removed in vacuo to yield 0.069 g (97%) of a black solid identified as **1-DEPE**. Anal. Calcd for C<sub>43</sub>H<sub>67</sub>N<sub>3</sub>P<sub>2</sub>Fe: C, 69.43; H, 9.08; N, 5.65. Found C, 69.29; H, 9.54; N, 5.28. <sup>1</sup>H NMR (benzene-*d*<sub>6</sub>):  $\delta$  0.32 (m, 8H, PCH<sub>2</sub>CH<sub>3</sub>), 0.42 (m, 12H, PCH<sub>2</sub>CH<sub>3</sub>), 0.66 (d, 6.1 Hz, 6H, CHMe<sub>2</sub>), 0.81 (sept, 6.1 Hz, 1H, P(CH<sub>2</sub>)<sub>2</sub>P), 1.01 (d, 6.1 Hz, 6H, CHMe<sub>2</sub>), 1.17 (sept, 7.6 Hz, 1H, P(CH<sub>2</sub>)<sub>2</sub>P), 1.27 (d, 6.1 Hz, 12H, CHMe<sub>2</sub>), 1.51 (m, 9.2 Hz, 1H, P(CH<sub>2</sub>)<sub>2</sub>P), 1.72 (s, 6H, C(Me)), 1.90 (sept, 7.6 Hz, 1H, P(CH<sub>2</sub>)<sub>2</sub>P), 2.73 (q, 7.6 Hz, 2H, CHMe<sub>2</sub>), 3.09 (q, 7.6 Hz, 2H, CHMe<sub>2</sub>), 7.06 (d, 7.6 Hz, 2H, *m*-pyridine or *p*-aryl), 7.16–7.23 (m, 4H, *m*-aryl), 7.39 (t, 7.6 Hz, 1H, *p*-pyridine), 8.27 (d, 7.6 Hz, 2H, *m*-pyridine or *p*-aryl). <sup>13</sup>C NMR (benzene-*d*<sub>6</sub>):  $\delta$  7.21–7.53 (dd, 17 Hz, 10.5 Hz, 135 Hz, PCH<sub>2</sub>CH<sub>3</sub>), 13.57–14.17 (dd, 57.5 Hz, 45.5 Hz, 197

(20) Pangborn, A. B.; Giardello, M. A.; Grubbs, R. H.; Rosen, R. K.; Timmers, F. J. *Organometallics* **1996**, *15*, 1518.



Hz, PCH<sub>2</sub>CH<sub>3</sub>), 20.35 (C(Me)), 22.72 (m, PCH<sub>2</sub>CH<sub>2</sub>P), 24.07 (CHMe<sub>2</sub>), 24.62 (CHMe<sub>2</sub>), 24.98 (CHMe<sub>2</sub>), 25.52 (CHMe<sub>2</sub>), 26.86 (CHMe<sub>2</sub>), 29.13 (CHMe<sub>2</sub>), 30.22 (m, PCH<sub>2</sub>CH<sub>2</sub>P), 113.26 (*m*-pyridine or *p*-aryl), 118.27 (*p*-pyridine), 123.42 (*m*-aryl), 124.11 (*m*-pyridine or *p*-aryl), 125.22 (*m*-aryl), 140.11, 143.71, 149.61, 151.52, 157.66. <sup>31</sup>P NMR (benzene-*d*<sub>6</sub>): δ 45.46, 77.01.

**Preparation of (iPrPDI)Fe(THT)(N<sub>2</sub>) (1-(THT)N<sub>2</sub>).** A 50-mL round-bottomed flask was charged with 0.130 g (0.219 mmol) 1-(N<sub>2</sub>)<sub>2</sub> and ~20 mL of pentane. The flask was fitted with a 180° needle valve, removed from the glovebox, and cooled to -78 °C. On the high-vacuum line, the contents of the flask were degassed. Two equivalents (excess) of tetrahydrothiophene were added to the flask by calibrated gas bulb. The resulting reaction mixture was warmed to room temperature and stirred for 1 h, during which time the olive green solution turned brownish-red. All of the volatiles were removed in vacuo to yield 0.137 g (95%) of a red-brown solid identified as 1-(THT)N<sub>2</sub>. Anal. Calcd for C<sub>37</sub>H<sub>51</sub>N<sub>3</sub>SFeN<sub>2</sub>: C, 71.02; H, 8.22; N, 6.72. Found C, 70.83; H, 8.08; N, 6.45. <sup>1</sup>H NMR (benzene-*d*<sub>6</sub>): δ -4.62 (s, 6H, C(Me)), 0.01 (d, 12H, CHMe<sub>2</sub>), 1.00 (s, 4H, THT), 1.28 (d, 12H, CHMe<sub>2</sub>), 2.28 (s, 4H, THT), 3.46 (q, 4H, CHMe<sub>2</sub>), 7.37 (d, 4H, *m*-aryl), 7.72 (t, 2H, *p*-aryl), 9.14 (t, 1H, *p*-pyridine), 10.97 (d, 2H, *m*-pyridine). IR (KBr): ν<sub>NN</sub> = 2045 cm<sup>-1</sup>.

**Preparation of (iPrPDI)Fe(PET<sub>3</sub>)(N<sub>2</sub>) (1-(PET<sub>3</sub>)N<sub>2</sub>).** A 20-mL scintillation vial was charged with 0.152 g (0.256 mmol) 1-(N<sub>2</sub>)<sub>2</sub> and ~10 mL of pentane. With stirring, 0.037 g (0.256 mmol) of triethylphosphine (PET<sub>3</sub>) was added to the vial via microsyringe. The addition induced a color change from olive green to bright grass green. The resulting reaction mixture was stirred for 1 h, after which time the volatiles were removed in vacuo to yield 0.165 g (98%) of 1-(PET<sub>3</sub>)N<sub>2</sub>. Anal. Calcd for C<sub>59</sub>H<sub>67</sub>N<sub>3</sub>P<sub>2</sub>Fe: C, 68.51; H, 8.55; N, 10.24. Found C, 68.87; H, 9.01; N, 9.92. <sup>1</sup>H NMR (benzene-*d*<sub>6</sub>): δ 0.75 (53.78), 1.06 (84.38), 2.07 (47.02), 7.89 (27.49). <sup>13</sup>C NMR (benzene-*d*<sub>6</sub>): δ 9.42 (PCH<sub>2</sub>CH<sub>3</sub>), 18.23 (PCH<sub>2</sub>-CH<sub>3</sub>), 25.24 (CHMe<sub>2</sub>), 25.90 (CHMe<sub>2</sub>), 28.14 (CHMe<sub>2</sub>), 113.58 (*m*-pyridine or *p*-aryl), 120.57 (*p*-pyridine), 124.35 *m*-aryl), 126.26 (*m*-pyridine or *p*-aryl), 149.30, 150.69. <sup>31</sup>P NMR (benzene-*d*<sub>6</sub>): δ 27.91 (-80 °C). <sup>15</sup>N NMR (benzene-*d*<sub>6</sub>): δ 330.23, 354.43. IR: ν<sub>NN</sub> = 2051 (pentane), 2028 cm<sup>-1</sup> (KBr).

**Preparation of (iPrPDI)Fe(NH<sub>2</sub><sup>t</sup>Bu) (1-(NH<sub>2</sub><sup>t</sup>Bu)).** A 50-mL round-bottomed flask was charged with 0.117 g (0.197 mmol) of

1-(N<sub>2</sub>)<sub>2</sub> and ~30 mL of pentane. The flask was fitted with a 180° needle valve, removed from the glovebox, and cooled to -78 °C. On the high-vacuum line, the contents of the flask were degassed. Using a calibrated gas bulb, 2 equiv (excess) of <sup>t</sup>BuNH<sub>2</sub> were added to the flask. The resulting reaction mixture was warmed to room temperature and stirred for 1 h, during which time the olive green solution turned red-brown. The volatiles were removed in vacuo to yield 0.106 g (88%) of a red-brown solid identified as 1-(NH<sub>2</sub><sup>t</sup>Bu). <sup>1</sup>H NMR (benzene-*d*<sub>6</sub>): δ -7.02 (s, 6H, C(Me)), 0.19 (s, 9H, <sup>t</sup>BuNH<sub>2</sub>), 0.25 (d, 6.1 Hz, 12H, CHMe<sub>2</sub>), 1.22 (d, 6.1 Hz, 12H, CHMe<sub>2</sub>), 2.53 (q, 7.6 Hz, 4H, CHMe<sub>2</sub>), 5.55 (s, 2H, <sup>t</sup>BuNH<sub>2</sub>), 7.31 (d, 7.6 Hz, 4H, *m*-aryl), 7.72 (t, 7.6 Hz, 2H, *p*-aryl), 8.87 (t, 7.6 Hz, 1H, *p*-pyridine), 11.50 (d, 6.1 Hz, 2H, *m*-pyridine). <sup>13</sup>C NMR (benzene-*d*<sub>6</sub>): δ 23.40 (CHMe<sub>2</sub>), 24.87 (CHMe<sub>2</sub>), 28.36 (CHMe<sub>2</sub>), 32.61 (<sup>t</sup>BuNH<sub>2</sub>), 41.83 (C(Me)), 61.26, 102.82 (*m*-pyridine or *p*-aryl), 124.98 (*m*-aryl), 125.80 (*m*-pyridine or *p*-aryl), 136.47, 143.57 (*p*-pyridine), 166.85, 167.71, 194.04. IR (KBr): ν<sub>NH</sub> = 3322 cm<sup>-1</sup>.

**Preparation of (iPrPDI)Fe(NCPh)<sub>2</sub> (1-(NCPh)<sub>2</sub>).** This molecule was prepared in a similar manner to 1-(DEPE) with 0.020 g (0.034 mmol) of 1-(N<sub>2</sub>)<sub>2</sub> and 4.0 μL of benzonitrile and yielded 0.019 g (71%) of a blue-green solid identified as 1-(NCPh)<sub>2</sub>. <sup>1</sup>H NMR (benzene-*d*<sub>6</sub>): δ -0.42 (d, 6.5 Hz, 12H, CH(CH<sub>3</sub>)<sub>2</sub>), 0.09 (s, 6H, C(CH<sub>3</sub>)<sub>2</sub>), 1.43 (d, 6.5 Hz, 12H, CH(CH<sub>3</sub>)<sub>2</sub>), 2.49 (sept., 6.5 Hz, 4H, CH(CH<sub>3</sub>)<sub>2</sub>), 6.37 (br s, 1H, *p*-phenyl), 6.45 (br s, 2H, *o*- or *m*-phenyl), 6.86 (br s, 2H, *o*- or *m*-phenyl), 7.60 (d, 7.5 Hz, 4H, *m*-aryl), 7.89 (t, 7.5 Hz, 2H, *p*-aryl), 8.87 (t, 8.5 Hz, 1H, *p*-pyr), 10.83 (d, 8.5 Hz, 2H, *m*-pyr).

**Acknowledgment.** We thank the Packard Foundation for support of this research. P.J.C. is a Cottrell Scholar supported by the Research Corporation and a Camille Dreyfus Teacher-Scholar.

**Supporting Information Available:** Crystallographic data for 1-(CN<sup>t</sup>Bu)<sub>2</sub>, 1-DEPE, 1-(PET<sub>3</sub>)N<sub>2</sub>, and 1-(THT)N<sub>2</sub> in cif format. This material is available free of charge via the Internet at <http://pubs.acs.org>.

IC700869H